

# Node-weighted measures for complex networks with directed and weighted edges for studying continental moisture recycling

D. C. ZEMP<sup>1,2</sup>, M. WIEDERMANN<sup>1,3</sup>, J. KURTHS<sup>1,3,4</sup>, A. RAMMIG<sup>1</sup> and J. F. DONGES<sup>1,5</sup>
<sup>1</sup> Potsdam Institute for Climate Impact Research - P.O. Box 60 12 03, 14412 Potsdam, Germany, EU

<sup>2</sup> Department of Geography, Humboldt University - Newtonstr. 15, 12489 Berlin, Germany, EU

<sup>3</sup> Department of Physics, Humboldt University - Newtonstr. 15, 12489 Berlin, Germany, EU

<sup>4</sup> Department of Control Theory, Nizhny Novgorod State University - Gagarin Avenue 23, 606950 Nizhny Novgorod, Russia

<sup>5</sup> Stockholm Resilience Centre, Stockholm University - Kräftriket 2B, 114 19 Stockholm, Sweden, EU

received 28 April 2014; accepted in final form 12 August 2014

published online 3 September 2014

PACS 89.75.-k – Complex systems

PACS 89.75.Hc – Networks and genealogical trees

PACS 92.60.Kc – Land/atmosphere interactions

**Abstract** – In many real-world networks nodes represent agents or objects of different sizes or importance. However, the size of the nodes is rarely taken into account in network analysis, possibly inducing bias in network measures and confusion in their interpretation. Recently, a new axiomatic scheme of node-weighted network measures has been suggested for networks with undirected and unweighted edges. However, many real-world systems are best represented by complex networks which have directed and/or weighted edges. Here, we extend this approach and suggest new versions of the degree and the clustering coefficient associated to network motifs for networks with directed and/or weighted edges and weighted nodes. We apply these measures to a spatially embedded network model and a real-world moisture recycling network. We show that these measures improve the representation of the underlying systems' structure and are of general use for studying any type of complex network.



Copyright © EPLA, 2014

**Introduction.** – In the course of the last decade complex network theory has become of great interest and has been widely applied in different domains including biology [1], communication [2], social science [3], economy [4] and climatology [5–8]. The systems of interest are modeled as networks with nodes representing agents (*e.g.*, cortical areas, topics in Wikipedia, locations on the Earth) and edges standing for interactions between them (*e.g.*, transmission of signals, hyperlinks, trades and statistical correlations). Several statistical measures have been developed to investigate the architecture of complex networks, *e.g.*, by counting neighbors or measuring the tendency to form triangles [9,10].

In most of the studies, nodes represent agents or objects of different sizes or importance (for example heterogeneity in demography among countries, in surface area among gridded data points and in capacity among airports). However, the size of the nodes is rarely taken into account in the network properties, which can induce bias and ambiguity in the network measures [11]. In climate networks [5,7,12], certain network measures

tend to artificially increase towards the poles due to a decrease in surface area represented by the nodes and thus an increase in node density [13]. Similarly, a region in the brain which is central with respect to its number of connections is not necessarily central when considering the volume of the brain it is connected to [11].

Recently, a novel framework for node-weighted network measures has been suggested based on the concept of “node-splitting invariance” (n.s.i.), *i.e.*, network measures unaffected by local aggregation or splitting of nodes [11]. Using node weights like volumes of the regions in brain networks, surface areas in climate networks, market values in world trade networks, sizes of the IP address space in the world-wide-web networks and article sizes in Wikipedia, the n.s.i. network measures improve the representation of the systems compared to their standard counterparts [11,13]. However, n.s.i. network measures have been suggested only for networks with undirected and unweighted edges so far. This means that connections are considered to be symmetric and edges are usually established between nodes if the strength of the connection

between them (for example statistical correlation in the case of climate networks) exceeds a certain threshold.

However, many real-world systems are best represented by networks with directed and/or weighted edges. Examples include world trade networks (with edge weights proportional to the amount traded with distinction between import and export), social networks (with edge weights proportional to the intensity of connection between people), air transport networks (with edge weights proportional to the number of available seats in flights between two airports) [14] and moisture recycling networks (with edge weight proportional to the amount of moisture transported between grid cells) [15].

In this work we use the n.s.i framework to suggest measures (degree, strength and clustering coefficient possibly associated with motifs) for networks with directed and/or weighted edges by assigning weights to all nodes in the network as well. We apply our novel measures to two spatially embedded networks in which node weights are proportional to surface areas that are represented by them: 1) a benchmark network model in which edge weights depend on the geographical distance between nodes (in consistency with a previous study on the length scales of moisture feedback) [16] and 2) a real-world network in which the edges represent direction and amount of moisture traveling from its source (evapotranspiration) to its final destination (precipitation) in South America. We show that the proposed n.s.i. measures improve the representation of the system compared to standard measures.

**Preliminaries.** – Consider a graph  $G = (V, E)$  with a given set of nodes  $V$ , edges  $E$  and the number of nodes  $|V| = N$ . Each node in the network is identified by a natural number  $i = 1, \dots, N$ .  $A = \{a_{ij}\} \forall i, j = 1, \dots, N$  is the adjacency matrix of size  $N \times N$  with  $a_{ij} = 1$  iff there is an edge connecting node  $i \in V$  and  $j \in V$  ( $i \neq j$ ) and  $a_{ij} = 0$  otherwise. If the network is directed (*i.e.*, the edges have a direction associated to them),  $A$  is in general not symmetric ( $a_{ij} \neq a_{ji}$ ) and  $a_{ij} = 1$  iff there is a directed edge originating from node  $i \in V$  and pointing towards node  $j \in V$  and zero otherwise. We can assign to each edge  $E_{ij}$  an intensive weight  $m_{ij} \in [0, 1]$  representing the strength of the dependency between nodes  $i$  and  $j$  and define an edge weight matrix  $M = \{m_{ij}\} \forall i, j = 1, \dots, N$  (from now on we omit  $\forall i, j = 1, \dots, N$ ). In this work we will present measures for different types of networks: binary undirected networks (BUN), edge-weighted undirected networks (WUN), binary directed networks (BDN) and edge-weighted directed networks (WDN).

In addition, we assign to each node  $i$  a positive and extensive weight  $w_i$  representing the size or importance of the node (sizes, surfaces, volumes, masses etc.) [11]. We define the total weight  $W = \sum_{i \in V} w_i$  as the node-weighted counterpart of the number of nodes  $N$ . A framework has been introduced that allows for the definition of node splitting invariant (n.s.i.) network measures which takes into account the weight of the nodes.

For transferring standard network measures to their n.s.i counterparts we follow a four step construction mechanism as described in [11]: a) sum up weights  $w_i$  whenever the original measure counts nodes or strengths, b) treat every node  $i \in V$  as if it were connected with itself, c) allow equality for  $i$  and  $j$  wherever the original measure involves a sum over distinct nodes  $i$  and  $j$  and d) “plug in” n.s.i. versions of measures wherever they are used in the definition of other measures. Step b) is needed because the twin nodes that result from a splitting of one given node are linked due to their similarity. As a result, the node resulting from the merging of the twin nodes is connected to itself [11]. To achieve this step, we connect each node to itself using the extended adjacency matrix  $A^+ = \{a_{ij}^+\}_{i,j \in V}$  with  $a_{ij}^+ = a_{ij}$  and  $a_{ii}^+ = 1$ . An equivalent extended edge weight matrix is not needed as it is common to assign a weight to the self-loops already which can be equal to zero if the node is not connected to itself.

**Definition of measures.** – In this section we will present some of the common local network measures  $f(G)$ , in particular the degree and clustering coefficient for networks with directed and/or weighted edges, and their n.s.i counterparts  $f^*(G)$ . Other global or local measures (*e.g.*, the betweenness centrality) can also be corrected using the n.s.i. framework [11] but will not be developed in this paper.



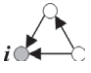
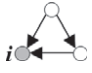
*Degree and strength.* The degree and its n.s.i counterpart called “area-weighted connectivity” in the context of spatially embedded networks has been described for BUN [5,11]. We generalize to the case of a directed network (BDN and WDN). For a node  $i$ , the in-degree  $k_i^{in} = \sum_{j \neq i} a_{ji}$  is the number of edges pointing towards  $i$  and the out-degree  $k_i^{out} = \sum_{j \neq i} a_{ij}$  is the number of edges originating from  $i$ . As these measures only count nodes, making them n.s.i. can be achieved by considering steps a), b) and c) in the construction mechanism. Hence,  $k_i^{in*} = \sum_{j \in V} w_j a_{ji}^+$  and  $k_i^{out*} = \sum_{j \in V} w_j a_{ij}^+$ . In the case of an undirected network (BUN and WUN), it is easy to see that the n.s.i degree is  $k_i^* = k_i^{in*} = k_i^{out*}$ .

For edge-weighted networks the concept of degree is extended to the one of strength. In a WDN, the in-strength  $s_i^{in} = \sum_{j \neq i} m_{ji}$  measures the total strength of edges pointing towards  $i$  and the out-strength  $s_i^{out} = \sum_{j \neq i} m_{ij}$  measures the total strength of edges originating from  $i$ . Using steps a), b) and c), the n.s.i. versions of these measures are  $s_i^{in*} = \sum_{j \in V} w_j m_{ji}$  and  $s_i^{out*} = \sum_{j \in V} w_j m_{ij}$ . If the network is not directed (WUN), we have  $s_i^* = s_i^{in*} = s_i^{out*}$ .

While the standard version of the in- and out-degree and the in- and out-strength can take integer values between 0 and  $N - 1$ , the n.s.i version of these measures can take real numbers between 0 and  $W$ .

*Clustering coefficient and motifs.* In simple networks (BUN), the clustering coefficient measures the tendency to form clusters or triangles formed by three connected nodes. It is defined as the ratio between the number of

Table 1: Network motifs taxonomy (“Mid.” stands for Middleman), patterns and the associated quantities used in the calculation of the directed clustering coefficients. On the left side, quantities that are used in the standard version:  $t_i$  is the number of triangles formed by  $i$ ,  $\tilde{t}_i$  is the edge-weighted counterpart of  $t_i$  and  $T_i$  is the maximum number of such triangles that  $i$  can form [14]. On the right side, the n.s.i versions of these quantities are given.

Tax.	Patterns	$t_i$	$\tilde{t}_i$	$T_i$	$t_i^*$	$\tilde{t}_i^*$	$T_i^*$
Cycle		$(A)_{ii}^3$	$(\hat{M})_{ii}^3$	$k_i^{in} k_i^{out} - k_i^{bil}$	$(A')_{ii}^3$	$(\hat{M}')_{ii}^3$	$k_i^{*in} k_i^{*out}$
Mid.		$(AA^T A)_{ii}$	$(\hat{M} \hat{M}^T \hat{M})_{ii}$	$k_i^{in} k_i^{out} - k_i^{bil}$	$(A' A'^T A')_{ii}$	$(\hat{M}' \hat{M}'^T \hat{M}')_{ii}$	$k_i^{*in} k_i^{*out}$
In		$(A^T A^2)_{ii}$	$(\hat{M}^T \hat{M}^2)_{ii}$	$k_i^{in} (k_i^{in} - 1)$	$(A'^T (A')^2)_{ii}$	$(\hat{M}'^T (\hat{M}')^2)_{ii}$	$(k_i^{*in})^2$
Out		$(A^2 A^T)_{ii}$	$(\hat{M}^2 \hat{M}^T)_{ii}$	$k_i^{out} (k_i^{out} - 1)$	$((A')^2 A'^T)_{ii}$	$((\hat{M}')^2 \hat{M}'^T)_{ii}$	$(k_i^{*out})^2$

triangles which involve the node  $i$  and the total number of triangles that  $i$  could have formed [14]:

$$C_i = \frac{\sum_{j \neq i} \sum_{h \neq (i,j)} a_{ij} a_{ih} a_{jh}}{k_i(k_i - 1)} = \frac{(A^3)_{ii}}{k_i(k_i - 1)}. \quad (1)$$

The n.s.i version of this measure obtained by using all four steps has already been suggested for BUN [11]:

$$C_i^* = \frac{\sum_{j \in V} \sum_{h \in V} w_j w_h a_{ij}^+ a_{ih}^+ a_{jh}^+}{(k_i^*)^2} = \frac{((A')^3)_{ii}}{w_i (k_i^*)^2}, \quad (2)$$

with  $A' = \{a_{ij}^+ w_j\}$ .

In the case of a WUN, one has to take into account the edge weights involved in the triangles. There are several ways to define the contribution of the triangle depending on the application of the network analysis. Here, in agreement with [14], we decide to take the geometric mean of the weights of the three involved edges. The clustering coefficient for edge-weighted networks is then

$$\tilde{C}_i = \frac{\sum_{j \neq i} \sum_{h \neq (i,j)} m_{ij}^{1/3} m_{ih}^{1/3} m_{jh}^{1/3}}{k_i(k_i - 1)} = \frac{(\hat{M}^3)_{ii}}{k_i(k_i - 1)}, \quad (3)$$

with  $\hat{M} = M^{[1/3]} = \{m_{ij}^{1/3}\}$ .

The n.s.i version of this measures then reads as

$$\tilde{C}_i^* = \frac{\sum_{j \in V} \sum_{h \in V} w_j w_h m_{ij}^{1/3} m_{ih}^{1/3} m_{jh}^{1/3}}{(k_i^*)^2} = \frac{((\hat{M}')^3)_{ii}}{w_i (k_i^*)^2}, \quad (4)$$

with  $\hat{M}' = \{(m_{ij})^{1/3} w_j\}$ .

In directed networks, the notion of cluster or triangle is replaced by the notion of network motifs [17]. Four types of network motifs have been emphasized depending on the direction of the edges involved in the triangle [14] (see table 1 for illustration). In the case of a BDN, the clustering coefficient of nodes  $i$  associated to a motif is defined as  $C_i = t_i/T_i$ , the fraction between the number of triangles  $t_i$  that belong to the particular motif actually

formed by  $i$  and the total number of triangles  $T_i$  of that motif that  $i$  could have formed [14]. The numerator  $t_i$  can be calculated by simple operations on the adjacency matrix  $A$  and the denominator  $T_i$  can be calculated by using the in-degree, out-degree and the bilateral degree ( $k_i^{bil} = \sum_{j \neq i} a_{ji} a_{ij}$  is the number of bilateral edges between  $i$  and its neighbors) (see table 1). This measure has been generalized for the case of WDN by taking into account the edge-weighted contribution of the triangles [14] and becomes  $\tilde{C}_i = \tilde{t}_i/T_i$ , where  $\tilde{t}$  is the edge-weighted counterpart of  $t$  and can be calculated by substituting the matrix  $A$  with the matrix  $\hat{M} = M^{[1/3]} = \{m_{ij}^{1/3}\}$ .

The n.s.i version of these measures becomes

$$C_i^* = \frac{t_i^*}{w_i T_i^*}, \quad (5a)$$

$$\tilde{C}_i^* = \frac{\tilde{t}_i^*}{w_i T_i^*}, \quad (5b)$$

where  $t_i^*$  is calculated by substituting  $A$  with  $A' = \{a_{ij}^+ w_j\}$  and  $A^T$  with  $A'^T = \{a_{ji}^+ w_j\}$ ,  $\tilde{t}^*$  by substituting  $\hat{M}$  with  $\hat{M}' = \{(m_{ij})^{1/3} w_j\}$  and  $\hat{M}^T$  with  $\hat{M}'^T = \{(m_{ji})^{1/3} w_j\}$  and  $T^*$  is obtained by substituting the in- and out-degree with their n.s.i counterparts as described above. The bilateral degree is no longer needed in the n.s.i version of the measure. In fact, it was subtracted in the denominator of the clustering coefficient for the motifs Cycle and Middleman in order to exclude the false triangles formed by a node and a pair of directed edges pointing to and originating from the same node [14]. In the n.s.i version of the clustering coefficient, a node connected to itself and bilaterally connected with another one forms a triangle and is accounted for in the clustering coefficient. All standard and n.s.i versions of the clustering coefficient can take values between 0 and 1.

**Application 1: benchmark network.** – In order to investigate the impact of the n.s.i correction on the network measures, we first construct an ensemble of 100

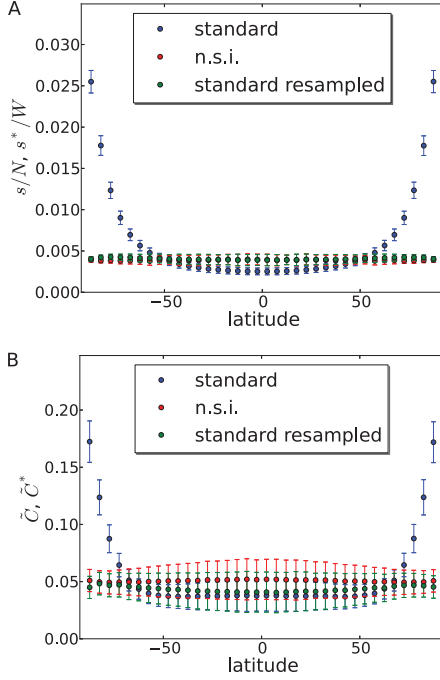


Fig. 1: (Colour on-line) Zonal averages (symbols) and standard deviations (error-bars) of the standard and n.s.i. versions of (A) the normalized strength and (B) the edge-weighted clustering coefficient applied to the benchmark edge-weighted and undirected network (WUN) model.

realizations of an undirected and edge-weighted (WUN) benchmark network model. Nodes represent grid cells which cover the global Earth surface (excluding the poles) with a spatial resolution of  $\Delta = 5^\circ$  in longitude and latitude resulting in a total number of  $N = 2592$ . This is a typical representative of grids found in many datasets used in climate and environmental sciences. The probability  $p_{ij}$  that node  $i$  and node  $j$  are linked is a function of the geodesic distance between them<sup>1</sup>. We assign to each edge a weight which is equal to the probability ( $m_{ij} = p_{ij}$ ). This relationship between the distance and the weights of the edges has been used in other benchmark networks [11] and is consistent with a previous study on the length scales of moisture feedback [16]. In this model which is perfectly homogeneous and isotropic, we expect the same network properties for all latitudes. To account for the irregular sampling, we assign to each node  $i \in V$  a weight which represents the size of the portion of the Earth's surface it covers:  $w_i = \cos(\text{latitude}_i)$  [5]. In addition, we construct another ensemble of this benchmark network model in which we pick randomly  $n_\lambda = \cos(\text{latitude}_\lambda) \cdot N$  nodes for each latitude  $\lambda$  (1654 nodes in total) such that the globe is covered approximately homogeneously as achieved in a previous study [18,19].

Figure 1 shows the zonal average of the standard and the n.s.i. version of strength and edge-weighted clustering

<sup>1</sup> $p_{ij} = \exp(-g_{ij}/\lambda)$  with  $\lambda$  representing the typical length scale and  $g_{ij}$  the geodesic distance between  $i$  and  $j$ . In this case we chose  $\lambda = 1110$  km to ensure an edge density of about 0.02.

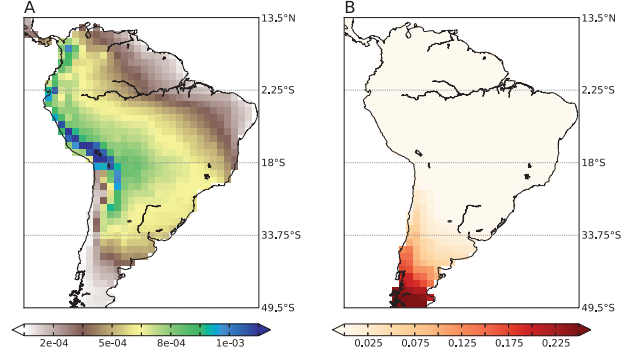


Fig. 2: (Colour on-line) (A) Normalized n.s.i. in-strength ( $s^{in*}/W$ ), (B) relative decrease of this measure compared to the standard version  $((s^{in}W - s^{in*}N)/s^{in}W)$ .

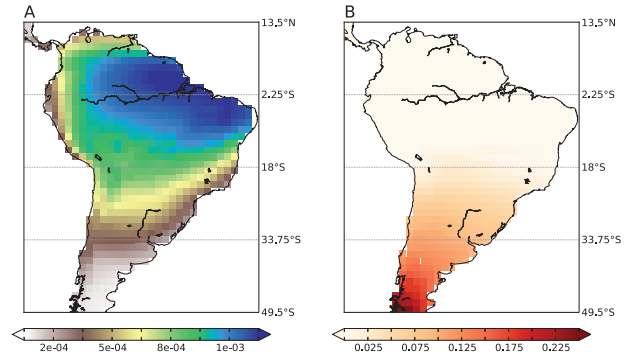


Fig. 3: (Colour on-line) (A) Normalized n.s.i. out-strength ( $s^{out*}/W$ ) and (B) relative decrease of this measure compared to the standard version  $((s^{out}W - s^{out*}N)/s^{out}W)$ .

coefficient applied to these benchmark networks averaged over all ensembles. The standard deviations of the clustering coefficient are larger than those of the strength due to finite size effect (*i.e.*, there are more neighbors than triangles). The standard strength and edge-weighted clustering coefficient  $\tilde{C}$  increase towards the poles. Regarding the strength, it is due to 1) a higher number of neighbors in this area and 2) higher weights of the edges connecting nodes at the poles. Regarding  $\tilde{C}$ , it is explained by 1) an increase in the probability that two neighbors of a node are also neighbors and 2) an increase in the weights of the edges involved in the triangles. This effect disappears after taking into account the surface covered by grid cells in different latitudes using the n.s.i. correction, as well as after sampling the nodes homogeneously on the globe. We note that for both measures, the first effect has been observed in the binary versions of the measures (degree and clustering coefficient) in a previous study [11]. However, the second factor is specific to edge-weighted networks as it is due to increasing weights of the edges due to a decreasing geodesic distance between nodes with increasing latitude. Thus, edge-weighted network measures experience systematic biases at latitudes higher than about  $50^\circ$  N or lower than  $50^\circ$  S due to increased node density which can be corrected using the n.s.i. versions of the measures. Sampling



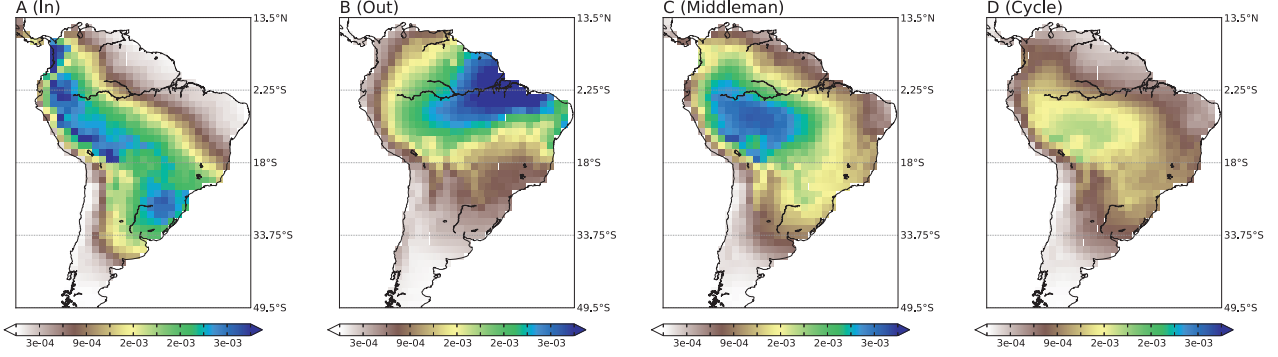


Fig. 4: (Colour on-line) n.s.i. edge-weighted and direct clustering coefficients  $\tilde{C}^*$  associated with the different network motifs.

networks homogeneously would also enable to fix these biases, but generally introduces an additional uncertainty. The n.s.i. correction has the advantage of directly avoiding such undesired operations.

#### Application 2: moisture recycling network. –

Next, we consider the output of the water accounting model-2 layers (WAM-2layers) [20] as a directed and edge-weighted complex network with self-interactions (WDN). WAM-2layers is forced by satellite data of hydrological cycle components and wind speed and diagnose the spatial distribution of atmospheric moisture from a certain location. The nodes in the network represent grid cells and the edges the direction and amount of water traveling from its source (evapotranspiration) to its final destination (precipitation). Grid cells are regularly distributed over the South American continent with a spatial resolution of 1.5 degree longitude and latitude, which leads to a total number of  $N = 681$  nodes. The weight  $m_{ij}$  of an edge pointing from node  $i$  to node  $j$  is the amount of moisture recycled from  $i$  to  $j$  (*i.e.*, evapotranspiration in  $i$  which precipitates in  $j$ ) and  $m_{ii}$  is the amount of locally recycled moisture. All the weights are normalized by the maximum amount of moisture recycled in the network such that  $0 < m_{ij} < 1 \forall i, j = 1, \dots, N$ . We note that the weights of the edges follow a similar relationship to the geodesic distances between nodes as modeled in the benchmark network. Again, to account for the irregular sampling, we assign to each node  $i$  a weight as in the benchmark network:  $w_i = \cos(\text{latitude}_i)$ .

The in- and out-strength have been rescaled to quantify, respectively, the fraction of precipitation that has been last evaporated from continental grid cells (fig. 2(A)) and the fraction of the evapotranspiration which precipitates in continental grid cells (fig. 3(A)). These measures highlight sources and sinks of continental moisture and are in agreement with a previous study on continental moisture recycling on the global scale [21]. Due to the increasing node density towards the South pole, there is an overestimation of up to 30% of these quantities (figs. 2(B) and 3(B)) in the southern part of South America which is corrected by the n.s.i. versions of these measures. Note that for out-strength the bias due to increasing

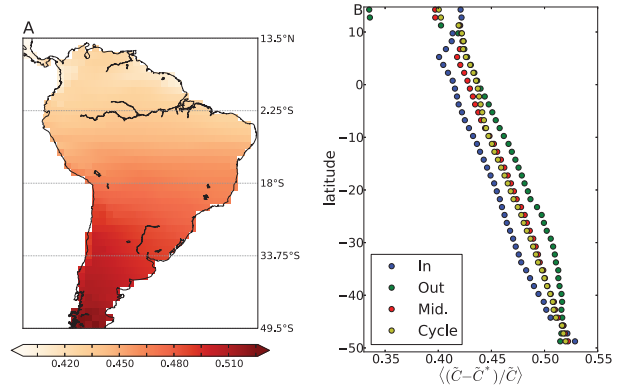


Fig. 5: (Colour on-line) Relative decrease in the edge-weighted clustering coefficient after n.s.i. correction  $(\tilde{C} - \tilde{C}^*)/\tilde{C}$  as observed in (A) a map for the motif Middleman and (B) zonal averages for all motifs.

node density towards the south pole extends significantly further northwards than for in-strength.

The n.s.i. edge-weighted clustering coefficient ( $\tilde{C}^*$ ) associated to the different motifs enables us a direct interpretation in terms of moisture flux. i)  $\tilde{C}^*$  associated with the motif “in” and “out” show regions which have the tendency to integrate and distribute moisture (figs. 4(A) and (B)). ii)  $\tilde{C}^*$  associated with the motif “Middleman” highlights intermediary regions involved in alternative pathways to the direct transport of moisture (fig. 4(C)). iii) If  $\tilde{C}^*$  is associated with the motif “Cycle”, high values indicate regions where moisture transport forms a closed loop, *i.e.*, where evapotranspiration returns as precipitation in the same grid cell after one precipitation-evaporation event (fig. 4(D)). Considered together, these results highlight the architecture of moisture recycling in South America. The eastern side of the Amazon basin is a source of moisture for the south-western part of the basin and the subtropical South America and moisture precipitates and evaporates on the way in the central-western part of the Amazon basin. However, the standard versions of the measure are overestimated in the southern part of South America where the node density increases. The n.s.i. versions are slightly decreasing compared to the

standard versions of the measures when approaching the Pole, indicating that the n.s.i. correction allows to get rid of this overestimation (fig. 5). We note that the use of the n.s.i. version has shifted the scale of the clustering coefficient.

In South America, the n.s.i. corrections do not lead to strong qualitative changes in the results of the presented measures because the southern part is dry and therefore there is little moisture transport south of 35° S. However on a global scale, moisture is transported from and into regions located close to the North pole [21]. Therefore, the use of n.s.i. versions of network measures provides significant qualitative and quantitative improvement of the representation of moisture recycling.

**Conclusion.** – In this work, we have developed new versions of some measures for directed and/or edge-weighted networks in order to take into account the weights of nodes. These measures respect the well-established criterion of node-splitting invariance (n.s.i.), which means that they are invariant with respect to local splitting or aggregation of nodes. These measures include the usual edge-weighted and/or directed degree but also clustering coefficient associated to different network motifs. In a first part we have given the standard and the n.s.i. versions of these measures and in a second part we have applied them to two different spatially embedded networks: 1) a benchmark network model which is undirected and edge-weighted on a global scale and 2) a real-world directed and edge-weighted moisture recycling network constructed using an atmospheric water tracking model over South America. In both networks we have assigned to each node a weight representing the surface area represented by it. We have shown that the use of our measures avoids systematic biases created by a higher node density and larger weights of the edges towards the poles. In the moisture recycling network there is little moisture transport from and to the southern part of South America. We argue that on global scale it should lead to a more accurate estimation of the contribution of export and import of continental moisture and to a better identification of key regions for the indirect transport of moisture. These improvements are possible because the heterogeneity of the size or the importance of nodes can be taken into account in the network analysis, which is not the case in most complex network studies. Therefore, we expect that the proposed measures might lead to important improvements in the analysis of many real-world complex systems such as chemical, neuronal, social, trade, climate, traffic or ecological networks.

\*\*\*

This paper was developed within the scope of the IRTG 1740/TRP 2011/50151-0, funded by the DFG/FAPESP. JFD acknowledges funding from the Stordalen Foundation and BMBF (project GLUES). The research of JK is partly supported by the grant No. 02.B.49.21.0003 with

Lobachevsky State University of Nizhny Novgorod. AR acknowledges funding from EU-FP7 AMAZALERT (raising the alert about critical feedbacks between climate and long-term land-use change in the Amazon) project, grant agreement No. 282664 and MW acknowledges funding from the IRTG 9751 and the German Federal Ministry for Science and Education via the BMBF Young Investigators Group CoSy-CC<sup>2</sup> (grant No. 01LN1306A). We thank R. J. VAN DER ENT for providing us with the model output, C.-F. SCHLEUSSNER for discussions and K. THONICKE for comments on the manuscript.

## REFERENCES

- [1] ZHOU C., ZEMANOVÁ L., ZAMORA G., HILGETAG C. C. and KURTHS J., *Phys. Rev. Lett.*, **97** (2006) 238103.
- [2] CAPOCCI A., SERVEDIO V. D. P., COLAIORI F., BURIOL L. S., DONATO D., LEONARDI S. and CALDARELLI G., *Phys. Rev. E*, **74** (2006) 036116.
- [3] NEWMAN M. E. and PARK J., *Phys. Rev. E*, **68** (2003) 036122.
- [4] BASKARAN T., BLÖCHL F., BRÜCK T. and THEIS F. J., *Int. Rev. Econ. Finance*, **20** (2011) 135.
- [5] TSONIS A. A., SWANSON K. L. and ROEBBER P. J., *Bull. Am. Meteorol. Soc.*, **87** (2006) 585.
- [6] YAMASAKI K., GOZOLCHIANI A. and HAVLIN S., *Phys. Rev. Lett.*, **100** (2008) 228501.
- [7] DONGES J. F., ZOU Y., MARWAN N. and KURTHS J., *EPL*, **87** (2009) 48007.
- [8] DONGES J. F., SCHULTZ H. C. H., MARWAN N., ZOU Y. and KURTHS J., *Eur. Phys. J. B*, **84** (2011) 635.
- [9] NEWMAN M. E. J., *SIAM Rev.*, **45** (2003) 167.
- [10] BOCCALETTI S., LATORA V., MORENO Y., CHAVEZ M. and HWANG D.-U., *Phys. Rep.*, **424** (2006) 175.
- [11] HEITZIG J., DONGES J. F., ZOU Y., MARWAN N. and KURTHS J., *Eur. Phys. J. B*, **85** (2012) 38.
- [12] GOZOLCHIANI A., YAMASAKI K., GAZIT O. and HAVLIN S., *EPL*, **83** (2008) 28005.
- [13] WIEDERMANN M., DONGES J. F., HEITZIG J. and KURTHS J., *EPL*, **102** (2013) 28007.
- [14] FAGIOLO G., *Phys. Rev. E*, **76** (2007) 026107.
- [15] ZEMP D. C., SCHLEUSSNER C.-F., BARBOSA H. M. J., VAN DER ENT R. J., DONGES J. F., HEINKE J., SAMPAIO G. and RAMMIG A., *Atmos. Chem. Phys. Discuss.*, **14** (2014) 1.
- [16] VAN DER ENT R. and SAVENIJE H., *Atmos. Chem. Phys.*, **11** (2011) 1853.
- [17] MILO R., SHEN-ORR S., ITZKOVITZ S., KASHTAN N., CHKLOVSKII D. and ALON U., *Science*, **298** (2002) 824.
- [18] GOZOLCHIANI A., HAVLIN S. and YAMASAKI K., *Phys. Rev. Lett.*, **107** (2011) 148501.
- [19] WANG Y., GOZOLCHIANI A., ASHKENAZY Y., BEREZIN Y., GUEZ O. and HAVLIN S., *Phys. Rev. Lett.*, **111** (2013) 138501.
- [20] VAN DER ENT R. J., WANG-ERLANDSSON L., KEYS P. W. and SAVENIJE H. H. G., *Earth Syst. Dyn. Discuss.*, **5** (2014) 281.
- [21] VAN DER ENT R. J., SAVENIJE H. H. G., SCHAEFLI B. and STEELE-DUNNE S. C., *Water Resour. Res.*, **46** (2010) W09525.